Insights to slip behavior on rough faults using discrete element modeling

Thomas Fournier[1] and Julia Morgan[1]

Received 4 April 2012; revised 25 May 2012; accepted 25 May 2012; published 22 June 2012.

[1] We simulate a range of fault slip behaviors using the discrete element method (DEM) to examine the controls on different slip modes on rough faults. Shear strain is imposed upon a 2-D bonded particle assemblage that contains a predefined fault. Slip modes on the fault vary from creep, to slow-slip, to stick-slip behavior, both spatially and temporally. The mode of slip is controlled largely by the local stress field along the fault, which depends on the local fault roughness. Portions of the fault that fail in relatively low normal stress regimes tend to slide continuously, whereas areas with high clamping stress produce stick-slip events. During stick-slip events, regions within the rupture zone that experience high slip are associated with physical asperities on the fault; ruptures terminate at barriers and through dissipation of the stored elastic energy. The simulated events show stress drops between 0.2–50 MPa, a slightly larger range than is inferred for natural earthquakes. Simulated events also have higher slip magnitudes than are observed during earthquakes for a given rupture length. The simulation produces many characteristics of fault behavior and is shown to be a successful avenue for future studies on the mechanics of fault slip. **Citation:** Fournier, T., and J. Morgan (2012), Insights to slip behavior on rough faults using discrete element modeling, *Geophys. Res. Lett.*, *39*, L12304, doi:10.1029/2012GL051899.

1. Introduction

[2] During large earthquakes, high slip regions are commonly regarded as asperities and are thought to correspond to strong patches along the fault [*Aki*, 1984; *Igarashi et al.*, 2003; *Resor and Meer*, 2009], which are able to support high shear stress. Several studies have pointed out the correlation between geometric structures on the fault and slip during earthquakes. *Resor and Meer* [2009] analyzed grooves and slickenlines on an exposed fault and found that, locally, slip direction is controlled by the topography of the fault. Also, slip magnitude distributions during earthquakes, as imaged by seismic inversion, show the same spatial correlation as fault roughness [*Candela et al.*, 2011]. This led *Candela et al.* [2011] to argue that slip distributions reflect the inherent roughness of the fault plane. It is clear that geometric features play a crucial role in earthquake mechanics, but it is not obvious how slip manifests as a result of fault topography. Additionally, stress concentration and evolution will be controlled by fault topography [*Schmittbuhl et al.*, 2006], however, how this process works, especially as it relates to fault zone damage [*Sagy and Brodsky*, 2009], remains an open question. Observing stress transfer in natural systems is difficult and understanding the evolution of these systems, over the full spectrum of fault slip, is challenged by the short record of seismicity and infrequent large earthquakes [e.g., *Pacheco et al.*, 1993]. In this study, we use discrete element method (DEM) simulations to look at processes that occur at the surface of a simulated 2-D fault to examine the effects of fault roughness and stress transfer in the distribution and mechanics of fault slip. We address how roughness translates to stress heterogeneity, which in turns affects slip mode.

[3] DEM simulations have been used successfully to examine the evolution of properties in granular fault gouge [*Morgan*, 1999, 2004; *Morgan and Boettcher*, 1999; *Abe et al.*, 2002; *Aharonov and Sparks*, 2004; *Guo and Morgan*, 2004, 2006; *Latham et al.*, 2006]. A range of slip modes, including stick-slip behavior, has been generated in DEM simulations [*Mora and Place*, 1994; *Scott*, 1996; *Place and Mora*, 1999; *Mora et al.*, 2000; *Hazzard et al.*, 2002; *Aharonov and Sparks*, 2004; *Hazzard and Young*, 2004; *Abe et al.*, 2006], and related to a variety of properties, such as changes in friction, driving strain rate, and gouge characteristics. Most of these studies however, examine system wide phenomena instead of discrete, local slip events that contribute to the observed behavior. A few studies have looked at seismicity produced by shearing the simulated material [*Hazzard and Young*, 2000, 2004], as well as the details of slip on a fault [*Scott*, 1996; *Place and Mora*, 1999; *Mora et al.*, 2000; *Hazzard et al.*, 2002]. Here, we look inside the fault zone to characterize individual slip events for cumulative slip, stress drop, and other quantities that can be compared to real systems. We find that slip mode is a direct response to stress on the fault, which, in the DEM simulations, is controlled by roughness, an important aspect of natural fault systems.

2. Earthquake Simulation

[4] We use the discrete element method described by *Guo and Morgan* [2004, 2006], where assigned interparticle contact parameters define the overall behavior of the particle assemblage. Continuum approximations of the bulk properties and behavior of the system are derived using the contact force distribution and displacement gradients [*Thornton and Barnes*, 1986; *Morgan and Boettcher*, 1999; *Oda and Iwashita*, 1999; *Morgan and McGovern*, 2005]. DEM simulations are ideal for fault studies because particle displacements are numerically unbounded, which allows for the accumulation of large strains. One advantage of DEM is

[1]Department of Earth Sciences, Rice University, Houston, Texas, USA.

Corresponding author: T. Fournier, Department of Earth Sciences, Rice University, 6100 Main St., MS 126, Houston, TX 77005, USA. (tomjfournier@gmail.com)

0094-8276/12/2012GL051899

Table 1. Model Parameters Used in the Simulation

		Shear Bond (MPa)*		Tensile Bond (MPa)*			
	Friction[a]	Mod.	Strength	Mod.	Strength	Density (kg/m^3)	Loading Velocity (m/s)
Wall Material	0.3	3e9	12e8	3e9	3e8	2500	-
Fault	0.1	-	-	-	-	-	-
Driving walls	0.3	3e9	12e8	3e9	3e8	2500	±0.15

[a]All values describe individual particle properties, bulk properties may differ.

that the system can be interrogated at many different scales, e.g., from the boundaries similar to a laboratory test, but also at the fault-scale, and grain scale, thus allowing for a detailed examination of the material evolution and mechanics.

[5] Our simulations are carried out in scaled 2-D domains, with final dimensions of 1 km length by ~0.5 km height. Approximately 15,000 particles with radii of 3 m and 4 m are consolidated between two horizontal walls to a normal stress of 100 MPa. Interparticle bonds are applied at all contacts, except along a prescribed horizontal fault surface within the domain (see auxiliary material); the material properties on either side of the fault are the same.[1] Model parameters are described in Table 1. Right lateral shear strain is imposed by moving the top and bottom walls in opposite directions at 15 cm/sec., while maintaining a constant normal stress. This model configuration can be thought of as a horizontal section through a strike-slip fault at depth, where the confining stress of 100 MPa would correspond to the normal stress on the fault at ~12 km depth, under lithostatic load and a Poisson's ratio of 0.25. Lateral periodic boundaries allow unlimited shear strains and prevent boundary effects. Simulations are initialized by applying a shear strain of ~27% (approximately 135 m of relative wall displacement), applied at a strain rate of 6e-4/s. The results presented here are from the time period following this initialization, where the boundary-driven strain rate is held constant for an additional 7% strain (120 sec.).

3. Results: Fault Slip Processes

[6] In general, simulated slip on the model fault initiates with a series of ruptures that span the entire interface. Following the initial rupture, the system evolves into a state characterized by periodic slip on shorter segments of the fault, with occasional large ruptures that break larger portions, but never the entire fault. We focus on the slip behavior during this post-initialization stage, which we interpret to be most representative of an active fault. Although we carried out several simulations, we examine the slip behavior in detail for one representative model here.

[7] Figure 1 shows an example of a dynamic (earthquake-like) slip event, characteristic of large events that occur during the simulation. Slip initiates in a region of high stress at ~700 m along the fault interface and propagates a distance of ~250 m. During fault slip, right lateral slip (denoted in red) occurs along the fault interface, while left lateral rebound (blue) occurs in the surrounding material, in response to the release of stored elastic energy. As slip accumulates over time, the locally high shear stress across the fault is relieved. In this example, the propagating rupture terminates to the left in a region of low differential stress, because there is insufficient stored energy for the rupture to continue, and to the right in a region of high stress, where the rupture

[1]Auxiliary materials are available in the HTML. doi:10.1029/2012GL051899.

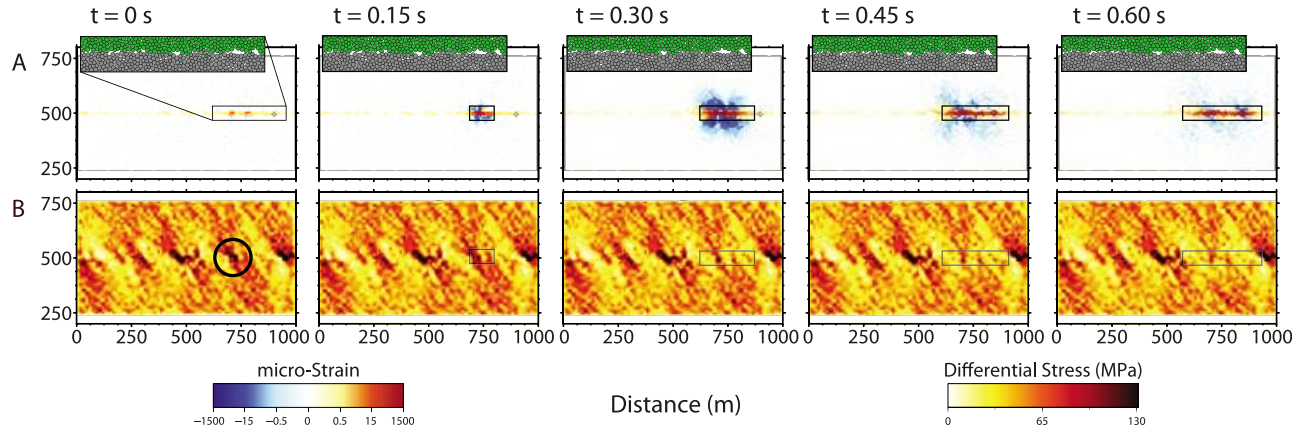

Figure 1. Sequence of snap shots at ~31.5% shear strain (4.5 cm of relative wall displacement between each snap shot), demonstrating a stick-slip event on the simulated fault. Columns 1 through 5 show the system state at consecutive time increments. (a) Instantaneous distortional strain (deviatoric strain invariant) field (red - right lateral shear strain, blue - left lateral shear strain); inset shows particle configuration in the rupture region. (b) Differential stress field showing regions of high shear stress spanning the fault. Slip originates in a high stress region (circled area in first column); shear stress dissipates locally as slip accumulates. The rectangles in snap-shots t = 0.15 − 0.6 highlight the slipping portion of the fault.

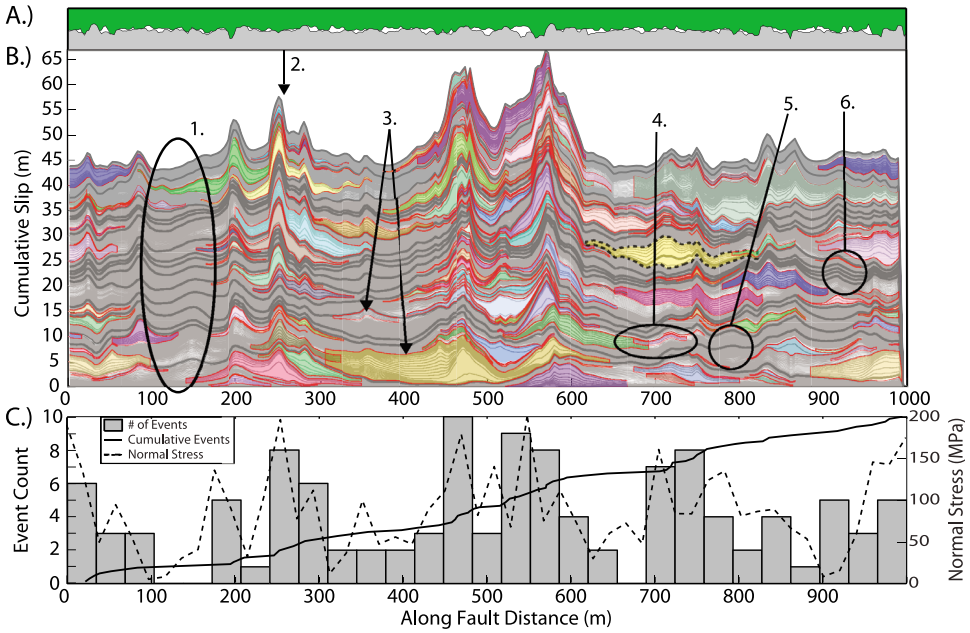

Figure 2. (a) Fault interface at 27% shear strain, revealing the rough nature of the interface (vertical exaggeration: 167%). (b) Cumulative slip through time along the fault. Individual dynamic events are identified by color; the colors are meaningless. The stick-slip example shown in Figure 1 is outlined with a black dashed line. Gray contour lines map the cumulative slip at each sampled time step (0.075 s, light gray) and each 100 time steps (7.5 s, dark gray). (c) Event statistics along the fault. Dynamic event counts (gray bars) are based on epicenter locations, binned at ~30 m intervals. Cumulative event curve (black line), normalized by 11.3, further delineates where epicenters are located. Normal stress on the fault (dashed line), averaged over the duration of the simulation, shows that high stresses correlate with repeating stick-slip events. See text for a description of annotations in Figure 2b.

energy is insufficient to break through the asperity. In this case, both features serve as barriers to rupture.

[8] In order to isolate the characteristics and causes of the slip behavior, we plotted slip along the fault as a function of time throughout the simulation (Figure 2). To do so, we sampled particles immediately adjacent to the fault (within 10 m on either side), and contoured their relative displacements with time. Cumulative fault slip is mapped in Figure 2b,

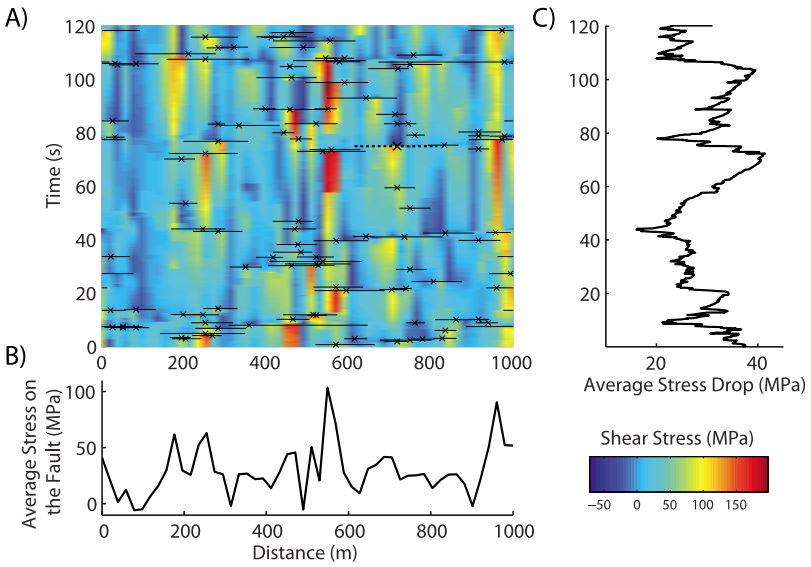

Figure 3. Spatial and temporal shear stress variations along the fault. (a) Shear stress binned over 20 m, plotted through time across the entire fault. Dynamic events are identified as black lines, indicating the extent of the rupture; X denotes hypocenter. (Dashed line and bold X indicates event shown in Figure 1). Shear stress builds slowly to its peak, and drops rapidly with rupture. (b) Shear stress along the fault, averaged over the simulation duration. Regions of highest stress correspond repeating stick-slip events. (c) Average stress drop through time across the entire fault length, denoting distinct episodes of rupture events, cascading along the fault.

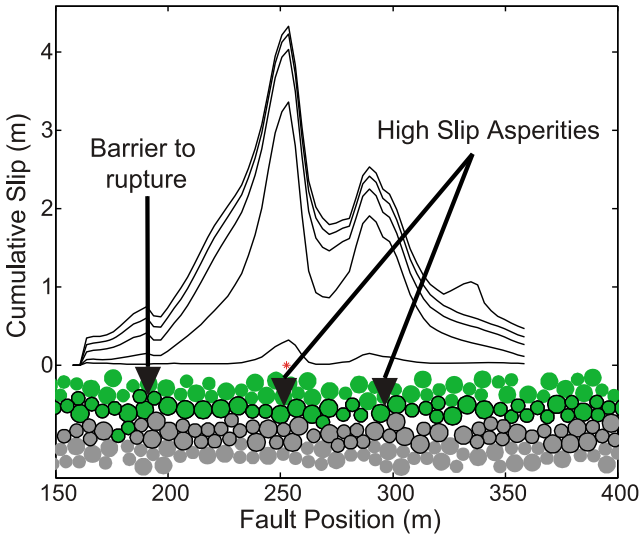

Figure 4. Slip distribution from typical medium sized event. Particle distribution along the rupture segment is shown at the base, the outlined particles indicate those used to identify earthquake like events. Epicenter is marked by a red asterisk, while black lines indicate the cumulative slip at each time-step in the sequence (0.075 sec/time-step).

showing a range of behaviors: continuous, creep-like behavior is indicated by uniformly spaced contours, denoting relatively low slip velocities; earthquake-like slip events show widely spaced contours, that taper laterally where rupture terminates. Simulated "earthquakes" are defined here by relative particle slip velocities of >2.5 m/s. Such events are then defined by origin time, rupture initiation point, length, cumulative slip distribution, stress drop, and duration. These earthquakes are highlighted in Figure 2b in color (colors are randomly assigned and have no meaning), showing remarkable spatial recurrence (although at irregular intervals). Intermediate slip behavior analogous to transient slow slip is also exhibited, when the background creep accelerates to some velocity below the "earthquake" threshold.

[9] Slip modes along the fault change temporally and spatially. A first-order comparison with the initial fault structure (Figure 2a), reveals a correlation between the distributions of slip modes and fault interface geometry. Earthquake-like events correspond to regions with persistent geometric asperities, which produce locally high shear stresses across the fault (Figure 2c). The different modes of slip behavior are annotated in Figure 2b. Zones of continuous creep correlate with low fault surface contact, accounting for low shear stresses observed (1). Events rupture nearly the same segment of the fault (2), much like repeating earthquakes recorded at many faults [e.g., *Nadeau et al.*, 1995; *Igarashi et al.*, 2003], There is a large range of event sizes produced in the simulation (3), seismic moment varies by 4 orders of magnitude. More complex slip behavior is also evident, for example, possible event triggering, where smaller events appear on the shoulders of large ones (4). Different creep velocities are observed, including accelerating and decelerating creep (5 and 6).

[10] The relationship between stress and slip behavior on the fault can be assessed by examining the local shear stress on the fault during the simulation. Stress tensors are calculated [*Morgan and McGovern*, 2005] for the narrow zone surrounding the fault surface (along 20 × 20 m pixels that span the fault), and plotted through time in Figure 3a. Shear stress varies both spatially and temporally, with certain regions (e.g., ∼200 m, ∼550 m, ∼950 m) consistently supporting higher stresses than elsewhere (Figure 3b). Stress is observed to gradually build up in specific areas until failure occurs, with rupture typically nucleating near the point of peak stress. The time-averaged shear stress along the fault (Figure 3b) correlates locally with the dominant mode of slip; regions that have high time-averaged shear stress show stick-slip behavior, whereas low time-averaged shear stress regions show creeping behavior. Stress variations averaged over the length of the fault allow the global stress drop to be calculated (Figure 3c), showing that distinct stress drops correspond with greater extents of rapid fault slip.

[11] Rapid (earthquake-like) events generally fall into two categories; 1) smaller events with simple rupture patterns and 2) larger events with complex ruptures. Small events involve a few particles that act as an asperity, while larger events occur when multiple asperities fail [e.g., *Abe et al.*, 2006]; their rupture patterns are complicated by the non-uniform timing and sequence of failures, resulting in bilateral and directional propagation and even "jumping" of the rupture front. Figure 4 shows the slip evolution of a medium sized event, which demonstrates the connection between fault asperities and slip in the simulations. In this example, the rupture is laterally confined, on the left by a neighboring asperity and on the right by dissipation of the energy into the surrounding material, analogous to the "barrier" and "asperity" models of *Aki* [1984], respectively.

[12] The complexity and variability of slip behavior even on a single, essentially planar (but rough) fault in these models demonstrates the richness of DEM simulations to recreate natural fault processes, as well as the potential for exploring the specific controls on fault behaviors that occur in natural fault systems. By using the synthetic earthquake catalog we are able to explore the event characteristics to see how well the simulation matches real earthquakes. We found 116 events based on the criteria outlined above. We find that the slip magnitude scales with the rupture length at about 1 m of slip for every 100 m of rupture, compared to real earthquakes that have ∼1 mm of slip for every 100 m of rupture [*Bodin and Brune*, 1996]. Stress drops averaged across the simulated rupture distance are between 0.2 and 50 MPa with peak stress drops as high as 100 MPa (Figure 3).

4. Discussion

[13] Our simulation results show that there is a strong correlation between local stress state and the type of slip that occurs on a given region of the fault. Although the regional stress field is imposed by the applied shear strain at the domain boundaries, the local stress is governed almost entirely by topography along the slip surface. Remarkably, despite the simplicity of our models, the slip modes produced in our simulation are very consistent with those observed on natural faults, including stick-slip, creep, and transient slow-slip, and these behaviors are persistent in regions where they are detected.

[14] We recognize that the main control on modeled slip behavior is fault roughness. In our simulations, fault roughness is defined by the particle dimensions and packing, controlling asperity size, distribution, and strength. The different behaviors along the fault correlate strongly with fault topography; local protrusions support high stress and produce stick slip events whereas in smooth regions or regions without fault contact, low normal stresses favors creep. Although the system is under a uniform applied load, the heterogeneous nature of the particle packing distributes the load unevenly at the fault interface [*Schmittbuhl et al.*, 2006], resulting in the observed variable slip behavior.

[15] We propose that real fault systems respond to similar controls to those modeled here; specifically, variations in slip mode reflect a heterogeneous stress field generated along a complex fault zone. We show that topographic features allow for variation in the shear strength of the fault which affects the slip mode (Figure 3), and that the slip distribution of an individual dynamic event is also related to the fault topography (Figure 4). In fact *Candela et al.* [2011] show that slip distributions determined from seismic inversion have a similar roughness structure as fault surface topography that is observed on exhumed faults. The scale of roughness in our models does not match that of natural faults [*Power et al.*, 1987; *Sagy et al.*, 2007; *Resor and Meer*, 2009; *Candela et al.*, 2011], mainly because fault roughness is observed over more than six orders of length scale, which is difficult to capture in these simulations. Nevertheless, it serves as a means to impart a heterogeneous stress field along the fault, and demonstrates the important role that roughness has on slip behavior. In natural fault systems, additional factors come into play that may have an important contribution to stress heterogeneity, including material heterogeneity (e.g., lithology, wall rock damage, porosity and resulting rheologic variations), pore fluids, and interacting faults.

[16] Our work suggests that variations in the base friction along the fault may not be the primary requirement to produce a wide spectrum of slip modes, as has been suggested by others [*Tajima and Kanamori*, 1985; *Scholz*, 1990; *Boatwright and Cocco*, 1996; *Igarashi et al.*, 2003]. This is because we use a constant interparticle coefficient of friction with no velocity or time dependence at the micro-scale. However, the resultant frictional behavior (i.e., at the macro scale) depends on other macroscale properties, e.g., particle packing, porosity, and contact area, all of which control the "state" of the material [*Morgan*, 2004]. The fact that multiple slip modes can arise from this comparatively simple particle scale description is intriguing, and offers new insights into the controls on fault slip behaviors.

[17] Qualitatively, our simulations show transitions from stable sliding to stick-slip behavior with increasing normal stress (Figure 2). The slip response in the system can be thought of as a phase transition between continuous sliding and stick-slip modes, controlled primarily by normal stress on the fault [e.g., *Dieterich*, 1978; *Aharonov and Sparks*, 2004]. Other studies have shown velocity dependence for similar slip mode transitions [e.g., *Nasuno et al.*, 1998]. The contacts that support higher than average normal stresses in our model exhibit stick-slip motion, whereas contacts with lower than average normal stress slide continuously; those contacts with normal stresses close to the phase transition show oscillatory behavior, where slip is periodic, but occurs at lower velocity and lasts longer than dynamic events (e.g., Figure 2b, mode 5).

5. Conclusions

[18] We have demonstrated the ability of DEM simulations to produce emergent slip behavior that mimics the range of fault slip modes in many ways, e.g., 1) a variety of slip behaviors are produced, including creep, oscillatory "slow-slip", and rapid earthquake-like rupture; 2) earthquake-like events show a self similar relationship for slip magnitude vs. length, and 3) stress drops are on the same order as those inferred for real earthquakes. The topographic features along the fault are the best predictors of slip behavior, because the fault structure directly affects the local stress field and therefore the slip behavior. The ability to study event types and their spatial and temporal relationships in this fully constrained system provides valuable insights into the processes active along real faults.

[19] **Acknowledgments.** The authors would like to thank two anonymous reviewers and NSF for their support, grant EAR-0711558.

[20] The Editor thanks two anonymous reviewers for assisting in the evaluation of this paper.

References

Abe, S., J. H. Dieterich, P. Mora, and D. Place (2002), Simulation of the influence of rate- and state-dependent friction on the macroscopic behavior of complex fault zones with the lattice solid model, *Pure Appl. Geophys.*, *159*(9), 1967–1983, doi:10.1007/s00024-002-8718-7.

Abe, S., S. Latham, and P. Mora (2006), Dynamic rupture in a 3-D particle-based simulation of a rough planar fault, *Pure Appl. Geophys.*, *163*(9), 1881–1892, doi:10.1007/s00024-006-0102-6.

Aharonov, E., and D. Sparks (2004), Stick-slip motion in simulated granular layers, *J. Geophys. Res.*, *109*, B09306, doi:10.1029/2003JB002597.

Aki, K. (1984), Asperities, barriers, characteristic earthquakes and strong motion prediction, *J. Geophys. Res.*, *89*(B7), 5867–5872, doi:10.1029/JB089iB07p05867.

Boatwright, J., and M. Cocco (1996), Frictional constraints on crustal faulting, *J. Geophys. Res.*, *101*(B6), 13,895–13,909, doi:10.1029/96JB00405.

Bodin, P., and J. N. Brune (1996), On the scaling of slip with rupture length for shallow strike-slip earthquakes: Quasi-static models and dynamic rupture propagation, *Bull. Seismol. Soc. Am.*, *86*(5), 1292–1299.

Candela, T., F. Renard, J. Schmittbuhl, M. Bouchon, and E. E. Brodsky (2011), Fault slip distribution and fault roughness, *Geophys. J. Int.*, *187*(2), 959–968, doi:10.1111/j.1365-246X.2011.05189.x.

Dieterich, J. H. (1978), Time-dependent friction and mechanics of stick-slip, *Pure Appl. Geophys.*, *116*(4–5), 790–806, doi:10.1007/BF00876539.

Guo, Y., and J. K. Morgan (2004), Influence of normal stress and grain shape on granular friction: Results of discrete element simulations, *J. Geophys. Res.*, *109*, B12305, doi:10.1029/2004JB003044.

Guo, Y., and J. K. Morgan (2006), The frictional and micromechanical effects of grain comminution in fault gouge from distinct element simulations, *J. Geophys. Res.*, *111*, B12406, doi:10.1029/2005JB004049.

Hazzard, J., and R. Young (2000), Simulating acoustic emissions in bonded-particle models of rock, *Int. J. Rock Mech. Min. Sci.*, *37*(5), 867–872, doi:10.1016/S1365-1609(00)00017-4.

Hazzard, J. F., and R. P. Young (2004), Dynamic modelling of induced seismicity, *Int. J. Rock Mech. Min. Sci.*, *41*(8), 1365–1376, doi:10.1016/j.ijrmms.2004.09.005.

Hazzard, J., D. Collins, W. Pettitt, and R. Young (2002), Simulation of unstable fault slip in granite using a bonded-particle model, *Pure Appl. Geophys.*, *159*(1–3), 221–245, doi:10.1007/PL00001252.

Igarashi, T., T. Matsuzawa, and A. Hasegawa (2003), Repeating earthquakes and interplate aseismic slip in the northeastern Japan subduction zone, *J. Geophys. Res.*, *108*(B5), 2249, doi:10.1029/2002JB001920.

Latham, S., S. Abe, and P. Mora (2006), Parallel 3-D simulation of a fault gouge using the lattice solid model, *Pure Appl. Geophys.*, *163*(9), 1949–1964, doi:10.1007/s00024-006-0106-2.

Mora, P., and D. Place (1994), Simulation of the frictional stick-slip instability, *Pure Appl. Geophys.*, *143*(1–3), 61–87, doi:10.1007/BF00874324.

Mora, P., D. Place, and S. Jaume (2000), Lattice solid simulation of the physics of fault zones and earthquakes: The model, results and directions, in *Geocomplexity and the Physics of Earthquakes*, *Geophys. Monogr.*

Ser., vol. 120, edited by J. B. Rundle, D. L. Turcotte, and W. Klein, pp. 105–126, AGU, Washington, D. C., doi:10.1029/GM120p0105.

Morgan, J. K. (1999), Numerical simulations of granular shear zones using the distinct element method: 2. Effects of particle size distribution and interparticle friction on mechanical behavior, *J. Geophys. Res.*, *104*(B2), 2721–2732, doi:10.1029/1998JB900055.

Morgan, J. K. (2004), Particle dynamics simulations of rate- and state-dependent frictional sliding of granular fault gouge, *Pure Appl. Geophys.*, *161*(9–10), 1877–1891, doi:10.1007/s00024-004-2537-y.

Morgan, J. K., and M. S. Boettcher (1999), Numerical simulations of granular shear zones using the distinct element method: 1. Shear zone kinematics and the micromechanics of localization, *J. Geophys. Res.*, *104*(B2), 2703–2719, doi:10.1029/1998JB900056.

Morgan, J. K., and P. J. McGovern (2005), Discrete element simulations of gravitational volcanic deformation: 2. Mechanical analysis, *J. Geophys. Res.*, *110*, B05403, doi:10.1029/2004JB003253.

Nadeau, R. M., W. Foxall, and T. V. McEvilly (1995), Culstering and periodic recurrence of microearthquakes on the San-Andreas Fault at Parkfield, California, *Science*, *267*(5197), 503–507, doi:10.1126/science.267.5197.503.

Nasuno, S., A. Kudrolli, A. Bak, and J. P. Gollub (1998), Time-resolved studies of stick-slip friction in sheared granular layers, *Phys. Rev. E*, *58*(2), 2161–2171, doi:10.1103/PhysRevE.58.2161.

Oda, M., and K. Iwashita (1999), *Mechanics of Granular Materials: An Introduction*, A. A. Balkema, Rotterdam, Netherlands.

Pacheco, J. F., L. R. Sykes, and C. H. Scholz (1993), Nature of seismic coupling along simple plate boundaries of the subduction type, *J. Geophys. Res.*, *98*(B8), 14,133–14,159, doi:10.1029/93JB00349.

Place, D., and P. Mora (1999), The lattice solid model to simulate the physics of rocks and earthquakes: Incorporation of friction, *J. Comput. Phys.*, *150*(2), 332–372, doi:10.1006/jcph.1999.6184.

Power, W. L., T. E. Tullis, S. R. Brown, G. N. Boitnott, and C. H. Scholz (1987), Roughness of natural fault surfaces, *Geophys. Res. Lett.*, *14*(1), 29–32, doi:10.1029/GL014i001p00029.

Resor, P. G., and V. E. Meer (2009), Slip heterogeneity on a corrugated fault, *Earth Planet. Sci. Lett.*, *288*(3–4), 483–491, doi:10.1016/j.epsl.2009.10.010.

Sagy, A., and E. E. Brodsky (2009), Geometric and rheological asperities in an exposed fault zone, *J. Geophys. Res.*, *114*, B02301, doi:10.1029/2008JB005701.

Sagy, A., E. E. Brodsky, and G. J. Axen (2007), Evolution of fault-surface roughness with slip, *Geology*, *35*(3), 283–286, doi:10.1130/G23235A.1.

Schmittbuhl, J., G. Chambon, A. Hansen, and M. Bouchon (2006), Are stress distributions along faults the signature of asperity squeeze?, *Geophys. Res. Lett.*, *33*, L13307, doi:10.1029/2006GL025952.

Scholz, C. H. (1990), *The Mechanics of Earthquakes and Faulting*, 2nd ed., Cambridge Univ. Press, Cambridge, U. K.

Scott, D. R. (1996), Seismicity and stress rotation in a granular model of the brittle crust, *Nature*, *381*(6583), 592–595, doi:10.1038/381592a0.

Tajima, F., and H. Kanamori (1985), Global survey of aftershock area expansion patterns, *Phys. Earth Planet. Inter.*, *40*(2), 77–134, doi:10.1016/0031-9201(85)90066-4.

Thornton, C., and D. J. Barnes (1986), Computer simulated deformation of compact granular assemblies, *Acta Mech.*, *64*(1–2), 45–61, doi:10.1007/BF01180097.